

AUTHOR QUERY FORM

	<p>Journal: Atomic Data and Nuclear Data Tables</p> <p>Article Number: 1110</p>	<p>Please e-mail or fax your responses and any corrections to:</p> <p>E-mail: corrections.essd@elsevier.river-valley.com</p> <p>Fax: +44 1392 285879</p>
---	---	---

Dear Author,

Please check your proof carefully and mark all corrections at the appropriate place in the proof (e.g., by using on-screen annotation in the PDF file) or compile them in a separate list. Note: if you opt to annotate the file with software other than Adobe Reader then please also highlight the appropriate place in the PDF file. To ensure fast publication of your paper please return your corrections within 48 hours.

For correction or revision of any artwork, please consult <http://www.elsevier.com/artworkinstructions>.

Location in article	Query / Remark click on the Q link to go Please insert your reply or correction at the corresponding line in the proof
Q1	Please confirm that given names and surnames have been identified correctly.
Q2	Fig. 1 is/are not cited in the text. Please check that the citation(s) suggested by the copyeditor is/are in the appropriate place, and correct if necessary.
Q3	The sentence 'Nuclei in....' has been amended. Please check and correct if necessary.
	<div style="border: 1px solid black; padding: 5px; display: inline-block;"> <p style="color: red; margin: 0;">Please check this box if you have no corrections to make to the PDF file</p> <input style="width: 30px; height: 20px; vertical-align: middle;" type="checkbox"/> </div>

Thank you for your assistance.



ELSEVIER

Contents lists available at SciVerse ScienceDirect

Atomic Data and Nuclear Data Tables

journal homepage: www.elsevier.com/locate/adt

NSE abundance data

a1 Andrzej Odrzywolek

M. Smoluchowski Institute of Physics, Jagiellonian University, Reymonta 4, 30-059 Krakow, Poland

ARTICLE INFO

Article history:

Received 23 July 2009

Received in revised form

16 August 2010

Accepted 29 March 2011

Available online xxx

ABSTRACT

A novel method of calculating nuclear statistical equilibrium (NSE) is presented. Basic equations are carefully solved using arbitrary precision arithmetic. A special interpolation procedure is then used to retrieve all abundances using tabulated results for neutrons and protons, together with basic nuclear data. Proton and neutron abundance tables, basic nuclear data, and partition functions for nuclides used in the calculations are provided. A simple interpolation algorithm using pre-calculated p and n abundances tabulated as functions of kT , ρ and Y_e is outlined. Unique properties of this method are: (1) ability to pick up out of NSE selected nuclei only, (2) computational time scaling linearly with number of re-calculated abundances, (3) relatively small amount of stored data: only two large tables, (4) slightly faster than solving the NSE equations using traditional Newton–Raphson methods for small networks (few tens of species); superior for huge (800–3000) networks, (5) does not require initial guess; works well on random input, (6) can be tailored to specific application, (7) ability to use third-party NSE solvers to obtain fully compatible tables, and (8) encapsulation of the NSE code for bug-free calculations. A range of applications for this approach is possible: covering tests of traditional NSE Newton–Raphson codes, generating starting values, code-to-code verification, and possible replacement of the old legacy procedures in supernova simulations.

© 2012 Elsevier Inc. All rights reserved.

E-mail address: andrzej.odrzywolek@uj.edu.pl.URL: <http://www.ribes.if.uj.edu.pl/>.

0092-640X/\$ – see front matter © 2012 Elsevier Inc. All rights reserved.

doi:10.1016/j.adt.2012.06.002

Contents

1. Introduction.....	2
2. NSE.....	2
2.1. Basic equations.....	2
2.2. Limitations of the Newton–Raphson NSE solvers.....	2
2.3. Interpolation algorithm.....	3
2.4. Discussion of NSE results.....	3
2.5. Properties of NSE.....	4
3. Proton and neutron NSE abundance table: explanation and examples of use.....	5
3.1. Implementation notes.....	5
4. Additional numerical data.....	6
Acknowledgments.....	6
Appendix. Supplementary data.....	6
References.....	6
Explanation of Tables.....	7
Table 1. Nuclei included in NSE and required nuclear data.....	7
Table 2. Temperature dependent partition function.....	7
Table 3. Proton and neutron abundance.....	7

1. Introduction

The main goal of the article is to provide a new method of computing the nuclear statistical equilibrium (NSE) abundances of the nuclear species. NSE for a vast range of conditions can be solved for $Y_e = 0.0, \dots, 1.0$, $\rho = 10^2, \dots, 10^{13}$ g/cc and $T = 2 \times 10^9, \dots, 10^{11}$ K covering almost any astrophysical situation imaginable. However, the particular method used to obtain example NSE datasets is not reliable under extreme conditions of the highest temperature and density. While this article does not concentrate on a particular target object, the results are useful for the study of pre-supernova stars after Si burning [1], thermonuclear supernovae [2], core-collapse [3], and protoneutron stars [4].

We calculate NSE abundances using a reliable arbitrary precision arithmetic approach. Tables of pre-calculated proton (X_p) and neutron (X_n) abundances as functions of the thermodynamic conditions defined by the triad ρ , T , Y_e are stored. Recovering of the remaining several hundred abundances from these two tables is a non-trivial task. Detailed description of the working procedure used to calculate the NSE abundances is provided. The algorithm is fast because of use of the pre-tabulated $X_{p,n}$. It has the unique ability to pick up out of the NSE ensemble only species of interest and other features. The computational time scales linearly with the number of required nuclides.

2. NSE

2.1. Basic equations

Well-known equations for the ensemble of $N_{iso} + 1$ nuclei in thermal equilibrium [5,6] are

$$\sum_{k=0}^{N_{iso}} X_k = 1, \quad (1a)$$

$$\sum_{k=0}^{N_{iso}} \frac{Z_k}{A_k} X_k = Y_e \quad (1b)$$

where the abundance X_k for k^{th} nuclei with atomic number Z_k and mass number A_k is

$$X_k = \frac{1}{2} G_k(T) \left(\frac{1}{2} \rho N_A \lambda^3 \right)^{A_k - 1} A_k^{5/2} X_n^{A_k - Z_k} X_p^{Z_k} e^{\frac{Q_k}{kT}}. \quad (2)$$

The temperature-dependent partition function for k^{th} nuclei is given by

$$G_k(T) = \sum_{i=0}^{i_{max}} (2J_{ik} + 1) e^{-\frac{E_{ik}}{kT}} \quad (3)$$

where summation is over all known excited states (numbered by the index i) of the k^{th} nucleus; J_{ik} and E_{ik} are the spin and the excitation energy, respectively; Q_k is the binding energy; ρ , T are the density and temperature of the plasma; N_A is Avogadro's number and k is the Boltzmann constant. The thermal De Broglie wavelength used in Eq. (2) is

$$\lambda = \frac{h}{\sqrt{2\pi m_H kT}} \quad (4)$$

where m_H is the mass of the hydrogen atom and h denotes Planck's constant (see Fig. 1).

The partition function has been calculated directly from a nuclear database using (3). Missing spins were assumed to be equal to zero. For uncertain data, the lowest value was used. Results are in good agreement with data used in Refs. [7,8], (see Fig. 2). For low temperatures ($kT \ll 0.5$ MeV) the partition function is simply equal to $2J + 1$ and both methods produce nearly identical results. For higher temperatures excited states contribute significantly (see Eq. (3) and Fig. 2). Unfortunately, NSE is applicable only in the high temperature region, and treatment of the partition function remains the most important source of uncertainty.

2.2. Limitations of the Newton–Raphson NSE solvers

The NSE equations, from a mathematical point of view, form a system of two large high-order polynomial equations (polynomial system) for unknown proton (X_p) and neutron (X_n) abundances. The system is solved numerically using the two-dimensional Newton–Raphson technique.¹ Due to large integer powers and other factors this approach is prone to numerous convergence problems. While in “normal” situations (typical thermodynamic parameters, good initial guess and standard selection of species) convergence of codes using machine floating point arithmetic

¹ In principle, the polynomial system might be reduced using Groebner basis methods, especially over rational field. In practice, an ensemble including protons, neutrons, ^4He , and single heavy nuclei can be solved, but additional components cause Groebner basis algorithms to fail in the sense of computational time: no result is returned in a period of several hours.

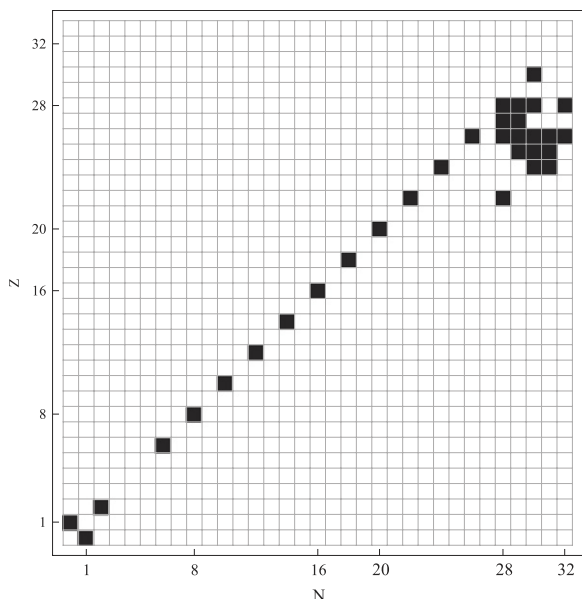


Fig. 1. Nuclides included in the NSE calculations. Much larger (800 nuclear species) networks were also tested.

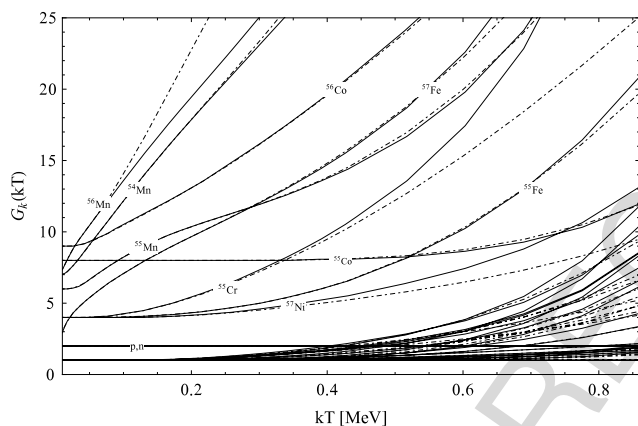


Fig. 2. Comparison of the partition functions derived directly using (3) and the database [9] (dot-dashed lines), and those from the Hix and Thielemann code [7,8] (solid lines). For low kT partitions both functions are identical, and begin to diverge for larger values of temperature.

is amazingly fast; failures are inevitable. Limited numerical precision might be a problematic issue. This forces programmers to include multi-level fail-safe procedures. They are by many orders of magnitude slower, and not guaranteed to converge. Careful programming with proper handling of round-off errors is required to get correct results, leading to additional complications. Due to problems with numerical precision and unpredictable iteration numbers, rapidly growing with number of species and for low temperatures, procedures are long, complicated and hard to parallelize.

Moreover, even if we are interested in abundance of a single nucleus the entire system (1) has to be solved. Such a situation is typical for neutrino spectrum calculations, where usually many more nuclear species are included in NSE than those with known neutrino emission rates. Usually very few of them contribute at a non-negligible level (e.g., p , ^{56}Ni , and ^{55}Co for ν_e emission at $Y_e = 0.5$). A large part of $kT - \rho - Y_e$ space is completely dominated by processes involving neutrons and protons only. In the course of research we have faced this problem. In a recent article [2] the NSE ensemble included 800 nuclides while the FFN

tables used include only 189 of them. Interpolation of the pre-calculated results has been found to be an optimal solution. Similar problems arise in core-collapse supernova simulations. Depending on temperature, NSE or the full reaction network is solved. Again, NSE can be computed for a larger ensemble, but due to limitations of network ODE solvers only a fraction of the species is traced.

2.3. Interpolation algorithm

To handle results of the NSE calculations efficiently, interpolation seems to be the wrong solution. Naively, one might try to interpolate stored X_p and X_n obtained from (1), and get X_k from (2). Unfortunately, this does not work. Even a very small inaccuracy in X_n or X_p produces enormous errors² in X_k due to large ($\sim A$) integer powers in (2). Another “brute force” method is tabulation of every X_k . This might be useful if a few of the NSE species are of interest. This is also the fastest approach. However, for larger number of species the amount of stored data becomes very large: tens or hundreds of tables like Table 3 (described below) instead of two. Fortunately, we have found a compromise, which successfully combines both ideas. The inability to get accurate abundances using interpolated X_n , X_p does not include grid points, because they can be stored with accuracy equal to the machine precision, or even better if required. First, we calculate the abundance of selected species X_k at grid points neighboring given a (ρ, T, Y_e) point. Next, we interpolate using computed X_k 's. Only proton and neutron abundances need to be tabulated, but more (using formula (2) at the eight corners of a cube) computational time is required compared to interpolation of stored X_k values for all nuclei. Additionally, the partition function $G_k(T)$, atomic and mass numbers Z_k, A_k , and binding energy Q_k have to be stored for all nuclei to use (2). Using (tri)linear interpolation Eqs. (1) are fulfilled automatically up to the original solving accuracy.

We still have to solve (1) to generate X_p and X_n tables. Any method (e.g., existing codes [10], pre-calculated results, or a web service [11]) may be used for this purpose. Because efficiency and speed of the code is not of primary importance if one uses an interpolating scheme, Eqs. (1a) and (1b) have been solved numerically using the MATHEMATICA code.³ An integrated MATHEMATICA [9] database has been used, including excited states and spins. This allows us to calculate the temperature-dependent partition function. Measured excited states were used if present in the database, otherwise they were neglected. Third party partition functions can be used as well. No Coulomb and screening corrections were applied.

Proton and neutron abundances are then tabulated as functions of temperature, density, and electron fraction. The NSE results are checked against available codes/results [10,11,13] with good agreement.

2.4. Discussion of NSE results

Determination of NSE abundances is crucial for many applications, including nucleosynthesis, neutrino emission, nuclear energy generation, and equation of state. Therefore we have

² This relative error can be estimated as $\delta(X_n^N X_p^Z) \sim A^2 \delta X$, where δX is the typical relative error of X_n (X_p) and A is the mass number. For $A \sim 60$ amplification of the relative error might be as large as 10^{18} (!) for $X_n \sim X_p \sim 0.5$.

³ The entire code [12] has approximately 100 lines including database loading, writing C headers, and solving (1) with arbitrary precision. The code is slow compared to FORTRAN equivalents, a price paid for arbitrary precision. This is not an important issue, because all we want is to generate tables. We do it once, in parallel if required. Later we use interpolators, which are very fast, even compared to codes using hardware floats.

Table A
Minimum number of nuclides required to compute all abundances above X_{min} .

X_{min}	Z	A	N_{iso}	Last included nuclide
10^{-1}	28	56	562	^{56}Ni
10^{-2}	28	57	563	^{57}Ni
10^{-4}	29	59	592	^{59}Cu
10^{-5}	30	60	620	^{60}Zn
10^{-6}	30	61	621	^{61}Zn
10^{-7}	30	63	623	^{63}Zn
10^{-8}	31	63	651	^{63}Ga
10^{-9}	31	65	653	^{65}Ga
10^{-10}	32	66	683	^{66}Ge
10^{-12}	32	68	685	^{68}Ge
10^{-20}	36	75	807	^{75}Kr
10^{-30}	41	87	970	^{87}Nb

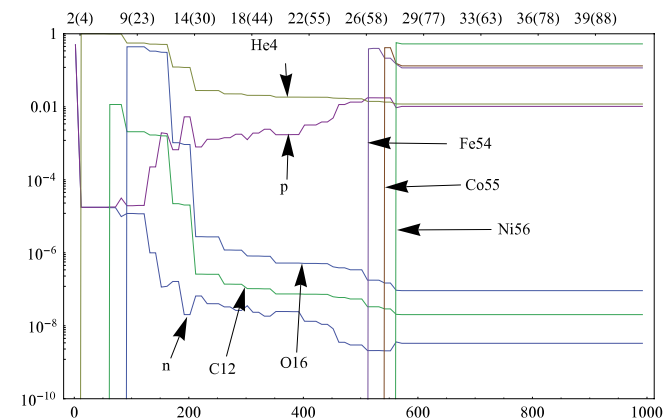


Fig. 3. NSE abundances as a function of the number of nuclei involved in calculations for $kT = 0.4$ MeV, $\rho = 10^7$ g/cm 3 and $Y_e = 0.5$.

made some tests to verify results and accuracy estimates. Despite known physical issues (temperature-dependent partition function, Coulomb corrections [13] and screening [14]) one of the most important factors is the number and selection of species included in Eqs. (1). Even a single important nuclei missing in the NSE ensemble may lead to radically different results. While inclusion of some species seems obvious (p , n , ^4He , ^{56}Ni , the iron group) further selection is more or less arbitrary.

To quantify the problem we tried to answer the following question: **what** is the maximum required atomic (Z) and mass number (A) to get a solution including all species with abundance larger than prescribed X_{min} ? The results are presented in Table A and Fig. 3. For example, from Table A, if we do not want to miss any of the species with abundance above, for example, 10^{-6} , we need at least nuclides up to ^{61}Zn . Nuclei in Fig. 3 are ordered according to Ref. [9]; **approximates** Z and A are included as tick marks for the top axis. This estimate gives an upper limit for the number of required nuclei. To get the true minimal number of nuclides required to get all species above the assumed accuracy one has to consider all subsets for the entire $kT - \rho - Y_e$ space considered. The number of subsets, given by the Bell number $B_{N_{iso}}$ is very large. Therefore, rigorous selection of species is impossible for large sets, and the safest thing to do is to use estimates given in Table A or consider all nuclei available [11]. In practice, however, other factors are decisive (e.g., limited computational resources in supernova simulations).

From Fig. 3 we conclude that the most primitive NSE including p and n only is not useful, except for very high temperatures (see Fig. 4). Inclusion of the alpha particle extends applications to lower temperatures but usually p and n abundances are wrong by a few orders of magnitude. To get the correct abundances of p and n for lower temperatures the iron peak has to be included. X_p and X_n are

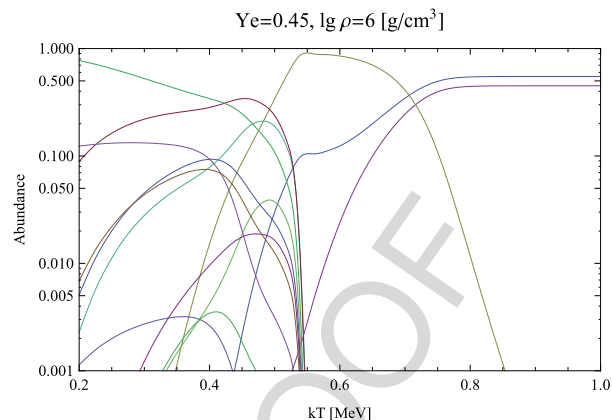


Fig. 4. NSE abundance versus temperature.

very stable if all nuclei below $Z = 28$, $A = 56$ are included. This number might be significantly reduced if we focus on a narrow Y_e range and exclude low mass ($A = 3, \dots, 16$) elements. Nevertheless, the results in Table A indicate that **not** more than 1000 nuclei are required to get all abundances above 10^{-30} . While it is possible to solve the NSE equations for more than 3000 nuclides [11], it does not change the results significantly.

2.5. Properties of NSE

We discuss here some properties of the NSE state for completeness. For very high temperatures,⁴ above $kT \simeq 0.5$ MeV in Fig. 4 ($T_9 \simeq 5.8$), no bound nuclei exist and we have a mixture of free neutrons and protons. In this case solution of the system of equations (1) is

$$X_n = 1 - Y_e, \quad X_p = Y_e.$$

If temperature decreases helium is being “synthesized” as in Big Bang nucleosynthesis. If temperature drops further, below $kT \simeq 0.35$ MeV ($T \simeq 4 \times 10^9$ K) and thermodynamic conditions are maintained for long enough, heavy, most-bound nuclei are preferred. Finally, a cold catalyzed matter state is pure ^{58}Fe (for $Y_e = 0.45$) (see Fig. 4); for $Y_e = 0.5$ it is ^{56}Ni . This is an appealing physical picture. Notice the extremely strong Y_e dependence of the NSE state (Fig. 5) for $0.35 < Y_e < 0.55$. The Y_e dependence for large temperatures is trivial: it is a smooth balance between p , n , and α abundances. The most interesting is the temperature range where heavy nuclei dominate. Note that for higher densities, the temperature threshold for heavy nuclei formation moves to higher temperatures (see Eq. (2) and footnote 4).

A striking feature of Fig. 5 is a rapid variation of the abundances within the range of $Y_e = 0.35, \dots, 0.55$ (Fig. 6). NSE prefers nuclei with individual $Y_e^{(k)} \equiv Z_k/A_k$ as close as possible to Y_e for the thermodynamic ensemble. For example, the double magic nuclei ^{78}Ni with largest known neutron excess⁵ (lowest $Y_e = 28/78 \simeq 0.36$) dominates for $Y_e < 0.365$ (not included in the example network) until neutrons (with $Y_e = 0$) become dominant. For the opposite behavior, $Y_e \gg 0.5$, protons are dominant.⁶

⁴ Actually, if we neglect the temperature-dependent partition function, according to Eq. (2), the solution depends on a factor proportional to ρ^2/kT^3 .

⁵ Neutron excess is equivalent to Y_e : $\eta = 1 - 2Y_e$.

⁶ Normally, for $Y_e \gg 0.5$ protons dominate. But if ^3Li would exist, it should take the role of hydrogen under NSE conditions if density is high enough. This species is still present in nuclide databases with atomic mass 3.030775 and binding energy 2.2676 MeV, despite the fact that experimental detection [15] has never been confirmed [16]; see also comments in ENSDF data at <http://ie.lbl.gov/ensdf/>.

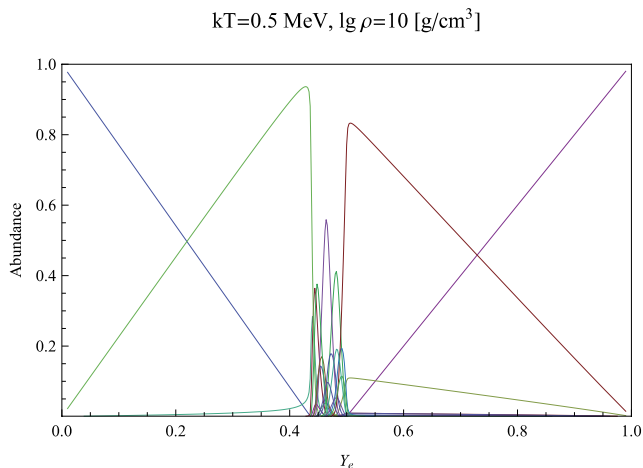


Fig. 5. NSE abundance versus electron fraction Y_e .

Note that for $Y_e = 0$, exact solution of the NSE equations is $X_n = 1$; for $Y_e = 1$ we get $X_p = 1$. Abundances for intermediate values of Y_e continuously approach these values for $Y_e \rightarrow 0$, and $Y_e \rightarrow 1$ (Fig. 5). Other abundances rapidly approach zero. Rapid abundance variation has a strong imprint on neutrino emission. For example, known for its large electron capture rate, ^{55}Co has non-negligible abundance only in narrow range of $Y_e = 0.47, \dots, 0.5$.

3. Proton and neutron NSE abundance table: explanation and examples of use

The dataset described and presented in this article is meant to be a simple example of the methods used. It is tailored to test against the 32-isotope NSE solver used by Garching group, based on serial code of Hix and Thielemann [7,8]. In real applications, larger tables should be used for the larger networks available online or generated (by request to the author) for a user-defined dataset tailored to the specific application.

Here we provide tables of the proton (X_p) and neutron (X_n) abundances, together with nuclear data required to calculate all remaining abundances, X_k . Additionally, a list of nuclides is required, including

1. atomic and mass numbers,
2. masses and binding energies, and

3. spins and excited states or, equivalently, the tabulated temperature-dependent partition function.

To calculate all NSE abundances we need basic nuclear data, presented in Table 1, and partition functions, from Table 2, with Table 3 showing X_p and X_n under NSE.

Using the approach presented here, the main computational cost is the calculation of the partition function, so use of the tabulated version instead of Eq. (3) is important. A detailed description of the algorithm is presented below. The goal is to calculate the abundance X_k of species k for given temperature T , density ρ , and Y_e ; $X_k = \text{NSE}(T, \rho, Y_e, k)$. For this we do the following:

1. from tables of the proton (neutron) abundance we pick up points surrounding the requested T, ρ, Y_e ; in the case of, for example, trilinear interpolation, these points are the 8 corners of a cuboid, the requested point must be inside or at the edge of the cuboid,
2. for all these points we calculate the abundance X_k , from (2),
3. now we have machine-precision accurate abundances X_i at the 8 corners of the cuboid, and
4. we interpolate (trilinear interpolation in the example) to get X_i at desired point.

We point out again that we interpolate X_k not X_p or X_n . X_k must be calculated exactly at grid points. An example implementation of the algorithm is included in the “libnse” library [17].

3.1. Implementation notes

This article deals with interpolation of the functions of three variables. Despite progress in computer hardware, available memory in particular, it is hard to find sophisticated 3D interpolators. Therefore trilinear, or mixed bilinear on the $T - \rho$ plane and staircase for Y_e , interpolations were used. A lot of computational time is spent on $X_p^Z X_n^{A-Z}$. The large integer power of the floating-point number can be computed nearly optimally using a double-exponentiation algorithm, usually included in standard math libraries. Minor improvements for the range of interest can be achieved using an optimal chain of powers, C++ template programming, or other techniques devoid of the `if` instruction.

We still recommend caution with integer powers of floating point numbers. For example, the standard “math.h” from C does not include integer powers, GNU Gsl has them only up to 9, while “cmath.h” from the C++ standard library does. This causes a large variation of the computational time. Higher-order interpolation

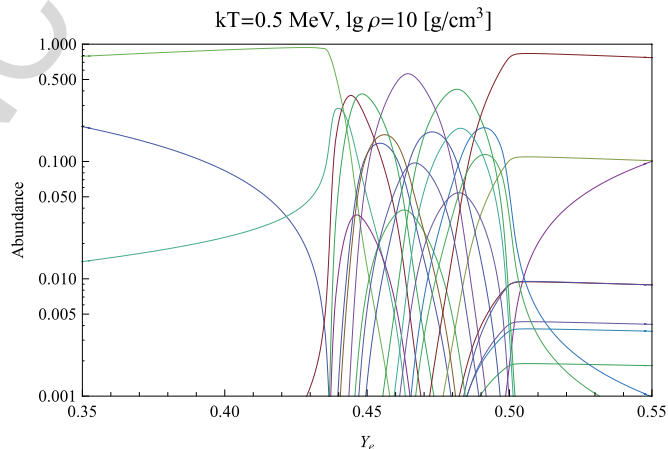


Fig. 6. Enlargement of a portion of Fig. 5 in the most interesting range of $Y_e = 0.35, \dots, 0.55$.

might possibly help to fit the procedure into CPU cache memory because of the reduced amount of data. However we are also in danger of overfitting, resulting in catastrophic errors, for example, negative abundances. If the amount of memory is not an issue, linear interpolation is recommended. The partition function is evaluated using linear interpolation.

4. Additional numerical data

The printed tables and results described in the article are meant to be simple examples of the proposed method. Extended versions of the tables, custom datasets, and numerical library can be downloaded from <http://ribes.if.uj.edu.pl/libnse/> or requested from the author. We also make available as supplemental material to this article extended versions of the tables.

Acknowledgments

I would like to thank P. Mach, T. Plewa, and K. Kifonidis for valuable discussions and verification of the NSE results, and an anonymous referee who helped to improve the final version of the article. The research was carried out with the supercomputer Deszno purchased, thanks to the financial support of the European Regional Development Fund in the framework of the Polish Innovation Economy Operational Program (contract no. POIG.02.01.00-12-023/08).

Appendix. Supplementary data

Supplementary material related to this article can be found online at <http://dx.doi.org/10.1016/j.adt.2012.06.002>.

References

- [1] A. Odrzywolek, A. Heger, *Acta Phys. Polon. B* 41 (2010) 1611.
- [2] A. Odrzywolek, T. Plewa, *Astron. Astrophys.* 529 (2011) A156.
- [3] A. Gawryszczak, J. Guzman, T. Plewa, K. Kifonidis, *Astron. Astrophys.* 521 (2010) A38.
- [4] A. Arcones, G. Martínez-Pinedo, L.F. Roberts, S.E. Woosley, *Astron. Astrophys.* 522 (2010) A25.
- [5] M.B. Aufderheide, I. Fushiki, S.E. Woosley, D.H. Hartmann, *Astrophys. J. Suppl.* 91 (1994) 389.
- [6] I.R. Seitenzahl, D.M. Townsley, F. Peng, J.W. Truran, *At. Data Nucl. Data Tables* 95 (2009) 96.
- [7] W.R. Hix, F.-K. Thielemann, *Astrophys. J.* 460 (1996) 869.
- [8] W.R. Hix, F.-K. Thielemann, *Astrophys. J.* 511 (1999) 862.
- [9] Wolfram Research Inc. MATHEMATICA 7.0 IsotopeData[.]. <http://reference.wolfram.com/mathematica/note/IsotopeDataSourceInformation.html>, 2008.
- [10] F.X. Timmes, Cococubed.com. http://cococubed.asu.edu/code_pages/nse.shtml, 2008.
- [11] B. Meyer, Webnucleo: NSE CALCULATOR. <http://www.webnucleo.org/pages/nse/0.1/>, 2008.
- [12] A. Odrzywolek, PSNS code. <http://th-www.if.uj.edu.pl/psns/>, 2005–2007.
- [13] I.R. Seitenzahl, F.X. Timmes, A. Marin-Lafleche, E. Brown, G. Magkotsios, J. Truran, *Astrophys. J. Lett.* 685 (2008) L129.
- [14] N. Itoh, F. Kuwashima, H. Munakata, *Astrophys. J.* 362 (1990) 620.
- [15] L.E. Williams, C.J. Batty, B.E. Bonner, C. Tschalär, H.C. Benöhr, A.S. Clough, *Phys. Rev. Lett.* 23 (1969) 1181.
- [16] D.R. Tilley, H.R. Weller, H.H. Hasan, *Nuclear Phys. A* 474 (1987) 1.
- [17] A. Odrzywolek, NSE library. <http://ribes.if.uj.edu.pl/libnse>, 2009–2010.

1 **Explanation of Tables****Table 1 Nuclei included in NSE and required nuclear data.**

No	position
Symbol	Standard element symbol
A	mass number
N	neutron number
Z	atomic number
Q	binding energy per nucleon [MeV]
J_0	ground state spin (0 if not known)

Table 2 Temperature dependent partition function.

NOTE: Without the ground state partition function $2J_0 + 1$, included in Table 3. Total partition function (3) is a sum of $2J_0 + 1$ and function tabulated below. Results are truncated below 10^{-6} .

No	position
Symbol	Standard element symbol
$kT = 0.2$	partition function for $kT = 0.2$ MeV
$kT = 0.4$	partition function for $kT = 0.4$ MeV
$kT = 0.6$	partition function for $kT = 0.6$ MeV
$kT = 0.8$	partition function for $kT = 0.8$ MeV
$kT = 1.0$	partition function for $kT = 1.0$ MeV

Table 3 Proton and neutron abundance

kT	temperature [MeV]
$\lg \rho$	base 10 logarithm of the density (g/cm^3)
Y_e	number of electrons per baryon
X_p	abundance of free protons
X_n	abundance of free neutrons

2

Table 1
Nuclei included in NSE and required nuclear data.

No	Symbol	Z	N	A	Q	J_0
1	^1_0n	0	1	1	0	1/2
2	^1_1H	1	0	1	0	1/2
3	^4_2He	2	2	4	7.0739150	0
4	$^{12}_6\text{C}$	6	6	12	7.6801440	0
5	$^{16}_8\text{O}$	8	8	16	7.9762060	0
6	$^{20}_{10}\text{Ne}$	10	10	20	8.0322400	0
7	$^{24}_{12}\text{Mg}$	12	12	24	8.2607090	0
8	$^{28}_{14}\text{Si}$	14	14	28	8.4477440	0
9	$^{32}_{16}\text{S}$	16	16	32	8.4931340	0
10	$^{36}_{18}\text{Ar}$	18	18	36	8.5199090	0
11	$^{40}_{20}\text{Ca}$	20	20	40	8.5513010	0
12	$^{44}_{22}\text{Ti}$	22	22	44	8.5335180	0
13	$^{50}_{22}\text{Ti}$	22	28	50	8.7556180	0
14	$^{48}_{24}\text{Cr}$	24	24	48	8.5722100	0
15	$^{54}_{24}\text{Cr}$	24	30	54	8.7779140	0
16	$^{55}_{24}\text{Cr}$	24	31	55	8.7318840	3/2
17	$^{54}_{25}\text{Mn}$	25	29	54	8.7379230	3
18	$^{55}_{25}\text{Mn}$	25	30	55	8.7649880	5/2
19	$^{56}_{25}\text{Mn}$	25	31	56	8.7383000	3
20	$^{52}_{26}\text{Fe}$	26	26	52	8.6095980	0
21	$^{54}_{26}\text{Fe}$	26	28	54	8.7363440	0
22	$^{55}_{26}\text{Fe}$	26	29	55	8.7465600	3/2
23	$^{56}_{26}\text{Fe}$	26	30	56	8.7903230	0
24	$^{57}_{26}\text{Fe}$	26	31	57	8.7702490	1/2
25	$^{58}_{26}\text{Fe}$	26	32	58	8.7922210	0
26	$^{55}_{27}\text{Co}$	27	28	55	8.6695750	7/2
27	$^{56}_{27}\text{Co}$	27	29	56	8.6948170	4
28	$^{56}_{28}\text{Ni}$	28	28	56	8.6427090	0
29	$^{57}_{28}\text{Ni}$	28	29	57	8.6709010	3/2
30	$^{58}_{28}\text{Ni}$	28	30	58	8.7320410	0
31	$^{60}_{28}\text{Ni}$	28	32	60	8.7807570	0
32	$^{60}_{30}\text{Zn}$	30	30	60	8.5832730	0

Table 2

Temperature-dependent partition function.

No	Name	0.20	0.40	0.60	0.80	1.00
3	⁴ He	0.00	0.00	0.00	0.00	0.00
4	¹² C	0.00	0.00	0.00	0.02	0.06
5	¹⁶ O	0.00	0.00	0.00	0.00	0.03
6	²⁰ Ne	0.00	0.08	0.34	0.72	1.21
7	²⁴ Mg	0.00	0.16	0.53	1.00	1.58
8	²⁸ Si	0.00	0.06	0.26	0.58	1.00
9	³² S	0.00	0.02	0.14	0.44	1.02
10	³⁶ Ar	0.00	0.04	0.21	0.61	1.37
11	⁴⁰ Ca	0.00	0.00	0.04	0.24	0.87
12	⁴⁴ Ti	0.02	0.38	1.32	3.09	5.90
13	⁵⁰ Ti	0.00	0.12	0.62	1.79	4.04
14	⁴⁸ Cr	0.12	0.85	1.98	3.60	5.95
15	⁵⁴ Cr	0.08	0.74	2.09	4.58	8.62
16	⁵⁵ Cr	1.39	5.48	11.30	18.60	27.00
17	⁵⁴ Mn	10.90	22.30	36.70	54.70	75.20
18	⁵⁵ Mn	4.36	7.81	14.00	24.00	37.40
19	⁵⁶ Mn	15.80	33.00	50.80	70.20	90.80
20	⁵² Fe	0.07	0.63	1.49	2.70	4.46
21	⁵⁴ Fe	0.00	0.19	1.11	3.43	7.57
22	⁵⁵ Fe	0.33	2.12	6.25	13.20	22.50
23	⁵⁶ Fe	0.07	0.68	2.01	4.78	9.60
24	⁵⁷ Fe	7.67	12.80	20.20	30.50	43.60
25	⁵⁸ Fe	0.09	0.87	2.81	6.71	13.10
26	⁵⁵ Co	0.00	0.07	0.74	2.86	7.02
27	⁵⁶ Co	4.07	10.60	18.50	27.90	38.50
28	⁵⁶ Ni	0.00	0.00	0.08	0.32	0.86
29	⁵⁷ Ni	0.14	1.04	2.46	4.63	7.87
30	⁵⁸ Ni	0.00	0.17	0.95	2.93	6.68
31	⁶⁰ Ni	0.00	0.25	1.31	3.89	8.48
32	⁶⁰ Zn	0.03	0.46	1.36	2.84	5.03

2

Table 3
Proton and neutron abundance table.

kT	$\lg \rho$	Y_e	X_p	X_n
0.20	6	0.350	1.4733451757175688e–32	1.9792286428615166e–01
0.20	8	0.350	4.6594595569570535e–37	1.9791728691182955e–01
0.20	10	0.350	1.4734610247732251e–41	1.9791672869601915e–01
0.40	6	0.350	7.6850895802764179e–10	2.0039781283597258e–01
0.40	8	0.350	2.5035658289594687e–14	1.9822605323795905e–01
0.40	10	0.350	7.9454130714268810e–19	1.9794846194430299e–01
0.60	6	0.350	8.6190577876701473e–03	3.0861905778717863e–01
0.60	8	0.350	1.6076815125584695e–06	2.0253972809389420e–01
0.60	10	0.350	5.3242575469851928e–11	1.9823081609598006e–01
0.80	6	0.350	3.4503551381543635e–01	6.4503551381543633e–01
0.80	8	0.350	6.0527987083834160e–03	3.0605116217065886e–01
0.80	10	0.350	5.6832537960862639e–07	1.9976073216155885e–01
1.00	6	0.350	3.4999839054511411e–01	6.4999839054511410e–01
1.00	8	0.350	1.6548297105954407e–01	4.6548297105954412e–01
1.00	10	0.350	1.5943665263060269e–04	2.1299547811356118e–01
0.20	6	0.400	4.5278905162835453e–32	8.3343373485753311e–02
0.20	8	0.400	1.4321164378624826e–36	8.3334338486210496e–02
0.20	10	0.400	4.5288358535831710e–41	8.3333433860011616e–02
0.40	6	0.400	2.2541535853182530e–09	8.7066391596373041e–02
0.40	8	0.400	7.6454369365453428e–14	8.3829450685805496e–02
0.40	10	0.400	2.4404642046330322e–18	8.3384805016069527e–02
0.60	6	0.400	1.3274703748466302e–02	2.1327470374824983e–01
0.60	8	0.400	4.5119825481078112e–06	9.0877967412558644e–02
0.60	10	0.400	1.6254313935731902e–10	8.3849904241914824e–02
0.80	6	0.400	3.9448770859198856e–01	5.9448770859198852e–01
0.80	8	0.400	9.4260257833551960e–03	2.0942531492521452e–01
0.80	10	0.400	1.6763122530124213e–06	8.6551386142692061e–02
1.00	6	0.400	3.9999820882445386e–01	5.9999820882445387e–01
1.00	8	0.400	2.0024502450742615e–01	4.0024502450742611e–01
1.00	10	0.400	3.8713189248855591e–04	1.0652457407487780e–01
0.20	6	0.450	1.2254155814326638e–15	1.0461956026905567e–14
0.20	8	0.450	1.3863583647470302e–17	1.0941992041239904e–16
0.20	10	0.450	1.5862580710493338e–19	1.1335873063097257e–18
0.40	6	0.450	1.3854242348476404e–05	8.6981272932959097e–05
0.40	8	0.450	1.6020742194861760e–07	8.9771845366122210e–07
0.40	10	0.450	1.6200879000788178e–09	1.0323858209007692e–08
0.60	6	0.450	2.3969925356851572e–02	1.2396992535682635e–01
0.60	8	0.450	2.6113737999714160e–04	3.6480691095702282e–03
0.60	10	0.450	5.0716727991727212e–06	2.4807585164625365e–05
0.80	6	0.450	4.4414588253856829e–01	5.4414588253856822e–01
0.80	8	0.450	1.7653064602620443e–02	1.1765299048431674e–01
0.80	10	0.450	2.7450088757524307e–04	1.5448501064190729e–03
1.00	6	0.450	4.4999809512767586e–01	5.4999809512767583e–01
1.00	8	0.450	2.4074257595157450e–01	3.4074257595157448e–01
1.00	10	0.450	2.6369076822919937e–03	2.3110858589751739e–02
0.20	6	0.500	2.1027565926622363e–06	3.3591508816189998e–23
0.20	8	0.500	2.0902933564115093e–07	3.9833138940328108e–26
0.20	10	0.500	2.1502284101490003e–08	4.5645516281556141e–29
0.40	6	0.500	2.4656257836791810e–02	1.1948909248170071e–07
0.40	8	0.500	2.9898277397867462e–03	1.2462253458017922e–10
0.40	10	0.500	2.7224923203959757e–04	1.6226416771168784e–13
0.60	6	0.500	5.5105593212499610e–02	5.5105593212499276e–02
0.60	8	0.500	2.7482483740179343e–02	6.7168188134800034e–05
0.60	10	0.500	6.4480794989162076e–03	3.9682763842094195e–08
0.80	6	0.500	4.9402975852718162e–01	4.9402975852718162e–01
0.80	8	0.500	4.6130285406649901e–02	4.6130284779868531e–02
0.80	10	0.500	2.1479785529572089e–02	3.4028673055878073e–05
1.00	6	0.500	4.9999805645135403e–01	4.9999805645135403e–01
1.00	8	0.500	2.8751054543310173e–01	2.8751054543310173e–01
1.00	10	0.500	3.0258682045056728e–02	2.9362486076929912e–03